

# Quadrupole transitions in the bound rotational-vibrational spectrum of the deuterium molecular ion

**Horacio Olivares Pilon**

Physique Quantique C.P. 165/82, and Physique Nucléaire Théorique et Physique Mathématique, C.P. 229, Université Libre de Bruxelles (ULB), B 1050 Brussels, Belgium

E-mail:

**Abstract.** After the study of the three body molecular system  $\text{H}_2^+$  (*J. Phys. B: At. Mol. Opt. Phys.* **45** 065101), its isotopomer, the deuterium molecular ion  $\text{D}_2^+$  is studied. The three-body Schrödinger equation is solved using the Lagrange-mesh method in perimetric coordinates. Energies and wave functions for four vibrational states  $v = 0 - 3$  and bound or quasibound states for total orbital momenta from 0 to 56 are calculated. The 1986 fundamental constant  $m_d = 3670.483014 m_e$  is used. The obtained energies have an accuracy from about 13 digits for the lowest vibrational state to at least 9 digits for the third vibrational excited state. Quadrupole transition probabilities per time unit between those states over the whole rotational bands were calculated. Extensive results are presented with six significant figures.

PACS numbers: 31.15.Ag, 31.15.Ac, 02.70.Hm, 02.70.Jn

Submitted to:

19 October 2018

## 1. Introduction

Despite of the simplicity of the molecular ion  $\text{H}_2^+$  and its isotopomers  $\text{D}_2^+$  and  $\text{T}_2^+$ , the three body Schrödinger equation can not be solved exactly. However, high precision results, for energies and wave functions, have been obtained using different approaches. For the particular case of the deuterium molecular ion, the ground state as well as some vibrational states are well known.

In this sense, non-adiabatic dissociation energies were calculated for several vibrational-rotational levels for the ground electronic state [1] and also in the first excited electronic state. In particular, the value of the ground state energy has been improved in several papers [2, 3, 4, 5]. Energies for the zero vibrational band for different values of the total angular momentum  $L$  have been also considered [6, 7]. Complete bound vibrational states below the dissociation limit  $v \leq 27$  were presented in [8] for the two lowest rotational quantum numbers  $L = 0, 1$ . Extension to this work until  $L = 2$  is presented in [9] but with a different value of the deuteron mass. Some expectation values have been also provided like the mean radii [7, 5] or quadrupole moments [7].

However, nowadays quadrupole transitions has not been considered for this system. In this paper, the E2 transitions are obtained from the three-body wave functions calculated with the Lagrange-mesh method in perimetric coordinates [10, 11, 7], with which the calculation is particularly simple and very precise. The Lagrange-mesh method is an approximate variational calculation using a basis of Lagrange functions and the associated Gauss quadrature. It has the high accuracy of a variational approximation and the simplicity of a calculation on a mesh.

In section 2, some expressions are presented but detailed explanations are given in [12]. In section 3, energies are given for the lowest four vibrational states over the full rotational bands and E2 transition probabilities are tabulated. Conclusions are presented in section 4. Throughout atomic units are used.

## 2. Lagrange-mesh calculation of transition probabilities

Quadrupole oscillator strength for an electric transition between an initial state  $i$  and a final state  $f$  is given by [13, 14]

$$f_{i \rightarrow f}^{(2)} = \frac{1}{30} \alpha^2 (E_f - E_i)^3 \frac{S_{if}^{(2)}}{2J_i + 1}, \quad (1)$$

where  $\alpha$  is the fine-structure constant and

$$S_{if}^{(2)} = S_{fi}^{(2)} = \sum_{M_i M_f \mu} |\langle \gamma_i J_i M_i | Q_\mu^{(2)} | \gamma_f J_f M_f \rangle|^2 = |\langle \gamma_i J_i || Q^{(2)} || \gamma_f J_f \rangle|^2, \quad (2)$$

is the reduced matrix element, defined according to [15]. Here,  $J_{i,f}$  is a total angular momentum,  $M_{i,f}$  is its projection and  $\gamma_{i,f}$  represents the other quantum numbers. The transition probability per time unit for  $E_f < E_i$  is given (the atomic unit of time is

$a_0/\alpha c \approx 2.4188843 \times 10^{-17}$  s) by

$$W_{i \rightarrow f}^{(2)} = \frac{1}{15} \alpha^5 (E_i - E_f)^5 \frac{S_{if}^{(2)}}{2J_i + 1}. \quad (3)$$

After the elimination of the center-of-mass motion, the system can be described using the Euler angles  $(\psi, \theta, \phi)$ , defining the orientation of the triangle formed by the three particles and three internal coordinates describing the shape of the triangle. The internal degrees of freedom are described using the perimetric coordinates  $(x, y, z)$  defined as

$$\begin{aligned} x &= R - r_{e2} + r_{e1}, \\ y &= R + r_{e2} - r_{e1}, \\ z &= -R + r_{e2} + r_{e1}, \end{aligned} \quad (4)$$

where  $r_{e1}$  and  $r_{e2}$  are the distances between the electron and deuterons 1 and 2, respectively. The domains of variation of these six variables are  $[0, 2\pi]$  for  $\psi$  and  $\phi$ ,  $[0, \pi]$  for  $\theta$  and  $[0, \infty[$  for  $x, y$  and  $z$ . In perimetric coordinates, the transition irreducible tensor operator  $Q_\mu^{(2)}$  is given by

$$\begin{aligned} Q_\mu^{(2)} &= \frac{1}{2} [R^2 - \gamma(2\zeta^2 - \rho^2)] D_{\mu 0}^2(\psi, \theta, \phi) - \sqrt{\frac{3}{2}} \gamma \zeta \rho [D_{\mu 1}^2(\psi, \theta, \phi) - D_{\mu -1}^2(\psi, \theta, \phi)] \\ &\quad - \sqrt{\frac{3}{8}} \gamma \rho^2 [D_{\mu 2}^2(\psi, \theta, \phi) + D_{\mu -2}^2(\psi, \theta, \phi)]. \end{aligned} \quad (5)$$

where

$$\gamma = 1 - \frac{2m_e}{M} - \frac{m_e^2}{M^2} \quad (6)$$

and the expression of  $R$ ,  $\rho$  and  $\zeta$  in terms of perimetric coordinates are given for example in [11, 12].

In order to evaluate (2) it is necessary to solve three-body Hamiltonian that involves Coulomb forces between the particles but no spin-dependent forces. The total orbital momentum  $L$  and parity  $\pi$  are constants of motion. The wave functions with orbital momentum  $L$  and parity  $\pi$  are expanded as [7]

$$\Psi_M^{(L\pi)\sigma} = \sum_{K=0}^L \mathcal{D}_{MK}^{L\pi}(\psi, \theta, \phi) \Phi_K^{(L\pi)\sigma}(x, y, z). \quad (7)$$

In practice, the sum can be truncated at some value  $K_{\max}$ . The normalized angular functions  $\mathcal{D}_{MK}^{L\pi}(\psi, \theta, \phi)$  are defined for  $K \geq 0$  by

$$\begin{aligned} \mathcal{D}_{MK}^{L\pi}(\psi, \theta, \phi) &= \frac{\sqrt{2L+1}}{4\pi} (1 + \delta_{K0})^{-1/2} [D_{MK}^L(\psi, \theta, \phi) \\ &\quad + \pi(-1)^{L+K} D_{M-K}^L(\psi, \theta, \phi)], \end{aligned} \quad (8)$$

where  $D_{MK}^L(\psi, \theta, \phi)$  represents a Wigner matrix element. They have parity  $\pi$  and change as  $\pi(-1)^K$  under permutation of the deuterons. The  $\Phi_K^{(L\pi)\sigma}$  functions with symmetry  $\sigma$  are symmetric for  $(-1)^K = \sigma\pi$  and antisymmetric for  $(-1)^K = -\sigma\pi$ , when  $x$  and  $y$  are

exchanged and are expanded in the Lagrange basis as

$$\begin{aligned} \Phi_K^{(L^\pi)\sigma}(x, y, z) = & \sum_{i=1}^N \sum_{j=1}^{i-\delta_K} \sum_{k=1}^{N_z} C_{Kijk}^{(L^\pi)\sigma} [2(1 + \delta_{ij})]^{-1/2} \\ & \times [F_{ijk}^K(x, y, z) + \sigma\pi(-1)^K F_{jik}^K(x, y, z)], \end{aligned} \quad (9)$$

where  $N$ ,  $N_z$  are the number of points in the  $x$  and  $z$ . Scale factors  $h$  and  $h_z$  are introduced in order to fit the meshes to the size of the physical problem (the same number  $N$  of mesh points and the same scale factor  $h$  are used for the two perimetric coordinates  $x$  and  $y$ ). Because of the symmetrization the sum over  $j$  is limited by the value  $i - \delta_K$ , where  $\delta_K$  is equal to 0 when  $(-1)^K = \sigma\pi$  and to 1 when  $(-1)^K = -\sigma\pi$ .

The three-body Hamiltonian in perimetric coordinates for each good quantum number  $L$  and its discretization on a Lagrange mesh are given in [11]. For given  $L^\pi$ , the eigenvalues in increasing order are labeled by a quantum number  $v \geq 0$  related to the vibrational excitation in the Born-Oppenheimer picture. The corresponding eigenvectors provide the coefficients appearing in expansion (9). Because the  $K$ -value appears in the eigenfunction (7), the matrix element (2) contains terms where  $K_f = K_i$ ,  $K_f = K_i \pm 1$  and  $K_f = K_i \pm 2$ . These terms are labeled as  $\kappa = 0, 1, 2$ , respectively (see [12]).

### 3. Energies and quadrupole transition probabilities

Using the Lagrange-mesh method, energies of the  $v = 0$  lowest vibrational bound states for some values of the total angular momentum from  $L = 0$  to 51 have been calculated in [7]. At the present study, those calculations are extended for all bound and quasibound states up to  $L = 56$  and four vibrational states  $v = 0 - 3$ . In order to calculate transition matrix elements involving two different wave functions, a single three-dimensional mesh is used for all the vibro-rotational states in consideration:  $N = N_x = N_y = 45$  and  $N_z = 20$ . A single set of scaling factors are also employed:  $h = h_x = h_y = 0.08$ ,  $h_z = 0.4$ . For a given  $K$  value, the total number of basis states is 20700 or 19800 depending on the parity of  $K$ . For  $K > 2$ , calculations are performed with  $K_{\max} = 2$ . They correspond to a size of 61200. Here, the 1986 fundamental constant  $m_d = 3670.483014 m_e$  is adopted and the dissociation energy is  $E_d = -0.499\,863\,815\,249$ .

Table 1 presents the energies obtained for the three lowest vibrational states  $v = 0 - 3$  as a function of the rotational quantum number. The accuracy is estimated from the stability of the digits with respect to calculations with  $N \pm 2$  mesh points. The error is expected to be at most of a few units on the last displayed digit. Comparisons when are available are displayed below at the same line for each  $L$ -value.

Table 1: Energies of the four lowest vibrational bound or quasibound states in the  $\Sigma_g$  rotational band of the  $D_2^+$  molecular ion. Quasibound states are separated from bound states by a horizontal bar. For each  $L$  value, the Lagrange-mesh results obtained with  $N_x = N_y = 45$ ,  $N_z = 20$  and  $h_x = h_y = 0.08$ ,  $h_z = 0.4$  are presented in the first line. Other references are indicated (<sup>a</sup>: [8], <sup>b</sup>: [4], <sup>c</sup>: [6], <sup>d</sup>: [1]). The deuteron mass is taken as  $m_d = 3670.483014 m_e$ .

$L$	$v = 0$	$v = 1$	$v = 2$	$v = 3$
0	-0.598 788 784 330 7	-0.591 603 121 903	-0.584 712 207 01	-0.578 108 591 4
	-0.598 788 784 330 68 <sup>a</sup>	-0.591 603 121 903 21 <sup>a</sup>	-0.584 712 207 009 99 <sup>a</sup>	-0.578 108 591 436 87 <sup>a</sup>
	-0.598 788 784 330 7 <sup>b</sup>	-0.591 603 121 903 2[4] <sup>b</sup>	—	—
	-0.598 788 784 32 <sup>d</sup>	-0.591 603 121 92 <sup>d</sup>	-0.584 712 206 99 <sup>d</sup>	-0.578 108 591 41 <sup>d</sup>
1	-0.598 654 873 220 5	-0.591 474 211 529	-0.584 588 169 62	-0.577 989 312 0
	-0.598 654 873 22 <sup>a</sup>	-0.591 474 211 53 <sup>a</sup>	-0.584 588 169 62 <sup>a</sup>	-0.577 989 311 96 <sup>a</sup>
	-0.598 654 873 220 5 <sup>b</sup>	-0.591 474 211 528 6[7] <sup>b</sup>	—	—
	-0.598 654 873 21 <sup>d</sup>	-0.591 474 211 53 <sup>d</sup>	-0.584 588 169 60 <sup>d</sup>	-0.577 989 311 98 <sup>d</sup>
2	-0.598 387 585 810 0	-0.591 216 909 624	-0.584 340 598 38	-0.577 751 241 9
	-0.598 387 585 809 98 <sup>c</sup>			
	-0.598 387 585 78 <sup>d</sup>	-0.591 216 909 63 <sup>d</sup>	-0.584 340 598 39 <sup>d</sup>	-0.577 751 241 91 <sup>d</sup>
3	-0.597 987 984 746 7	-0.590 832 247 071	-0.583 970 493 74	-0.577 395 352 5
	-0.597 987 984 746 72 <sup>c</sup>			
	-0.597 987 984 75 <sup>d</sup>	-0.590 832 247 09 <sup>d</sup>	-0.583 970 493 75 <sup>d</sup>	-0.577 395 352 53 <sup>d</sup>
4	-0.597 457 646 783 8	-0.590 321 753 376	-0.583 479 339 94	-0.576 923 084 8
	-0.597 457 646 783 78 <sup>c</sup>			
	-0.597 457 646 78 <sup>d</sup>	-0.590 321 753 37 <sup>d</sup>	-0.583 479 339 94 <sup>d</sup>	-0.576 923 084 78 <sup>d</sup>
5	-0.596 798 642 700 8	-0.589 687 437 079	-0.582 869 085 94	-0.576 336 330 6
	-0.596 798 642 700 81 <sup>c</sup>			
	-0.596 798 642 68 <sup>d</sup>	-0.589 687 437 09 <sup>d</sup>	-0.582 869 085 95 <sup>d</sup>	-0.576 336 330 45 <sup>d</sup>
6	-0.596 013 511 469 5	-0.588 931 760 548	-0.582 142 120 82	-0.575 637 408 9
	-0.596 013 511 469 53 <sup>c</sup>			
7	-0.595 105 229 402 0	-0.588 057 609 916	-0.581 301 244 47	-0.574 829 037 2
	-0.595 105 229 401 95 <sup>c</sup>			
8	-0.594 077 175 129 3	-0.587 068 260 974	-0.580 349 634 45	-0.573 914 299 3
	-0.594 077 175 129 31 <sup>c</sup>			
9	-0.592 933 091 328 5	-0.585 967 341 945	-0.579 290 809 74	-0.572 896 610 0
	-0.592 933 091 328 53 <sup>c</sup>			
10	-0.591 677 044 141 4	-0.584 758 794 049	-0.578 128 592 47	-0.571 779 678 0

Continued on Next Page...

Table 1 – Continuation

$L$	$v = 0$	$v = 1$	$v = 2$	$v = 3$
	-0.591 677 044 141 33 <sup>c</sup>			
11	-0.590 313 381 220 4	-0.583 446 830 801	-0.576 867 068 41	-0.570 567 467 4
	-0.590 313 381 220 32 <sup>c</sup>			
12	-0.588 846 689 292 3	-0.582 035 896 884	-0.575 510 547 15	-0.569 264 159 6
	-0.588 846 689 292 25 <sup>c</sup>			
13	-0.587 281 752 056 3	-0.580 530 627 415	-0.574 063 522 70	-0.567 874 114 7
14	-0.585 623 509 141 9	-0.578 935 808 297	-0.572 530 635 17	-0.566 401 834 8
15	-0.583 877 016 744 9	-0.577 256 338 258	-0.570 916 634 23	-0.564 851 928 8
16	-0.582 047 410 445 6	-0.575 497 193 053	-0.569 226 344 58	-0.563 229 078 7
17	-0.580 139 870 600 8	-0.573 663 392 212	-0.567 464 634 07	-0.561 538 010 0
18	-0.578 159 590 589 4	-0.571 759 968 586	-0.565 636 384 50	-0.559 783 462 5
19	-0.576 111 748 091 6	-0.569 791 940 871	-0.563 746 465 33	-0.557 970 166 4
20	-0.574 001 479 489 6	-0.567 764 289 167	-0.561 799 710 40	-0.556 102 819 0
21	-0.571 833 857 401 5	-0.565 681 933 603	-0.559 800 897 57	-0.554 186 066 4
22	-0.569 613 871 292 8	-0.563 549 715 941	-0.557 754 731 37	-0.552 224 486 3
23	-0.567 346 411 059 8	-0.561 372 384 075	-0.555 665 828 34	-0.550 222 575 0
24	-0.565 036 253 438 8	-0.559 154 579 261	-0.553 538 705 16	-0.548 184 735 6
25	-0.562 688 051 068 4	-0.556 900 825 932	-0.551 377 769 16	-0.546 115 270 0
26	-0.560 306 324 011 5	-0.554 615 523 892	-0.549 187 311 26	-0.544 018 372 2
27	-0.557 895 453 538 2	-0.552 302 942 710	-0.546 971 501 01	-0.541 898 124 2
28	-0.555 459 677 964 5	-0.549 967 218 120	-0.544 734 383 64	-0.539 758 493 9
29	-0.553 003 090 349 8	-0.547 612 350 239	-0.542 479 878 85	-0.537 603 334 2
30	-0.550 529 637 862 4	-0.545 242 203 435	-0.540 211 781 30	-0.535 436 385 0
31	-0.548 043 122 635 1	-0.542 860 507 670	-0.537 933 762 62	-0.533 261 275 0
32	-0.545 547 203 949 6	-0.540 470 861 200	-0.535 649 374 77	-0.531 081 527 3
33	-0.543 045 401 606 3	-0.538 076 734 487	-0.533 362 054 69	-0.528 900 563 8
34	-0.540 541 100 352 2	-0.535 681 475 235	-0.531 075 130 31	-0.526 721 713 7
35	-0.538 037 555 267 4	-0.533 288 314 477	-0.528 791 827 57	-0.524 548 221 2
36	-0.535 537 898 025 9	-0.530 900 373 673	-0.526 515 278 89	-0.522 383 256 3
37	-0.533 045 143 977 9	-0.528 520 672 798	-0.524 248 532 76	-0.520 229 927 0
38	-0.530 562 200 023 2	-0.526 152 139 463	-0.521 994 564 82	-0.518 091 292 9
39	-0.528 091 873 277 5	-0.523 797 619 127	-0.519 756 290 58	-0.515 970 382 5
40	-0.525 636 880 568 4	-0.521 459 886 554	-0.517 536 580 00	-0.513 870 212 6
41	-0.523 199 858 840 0	-0.519 141 658 708	-0.515 338 274 50	-0.511 793 812 4
42	-0.520 783 376 595 1	-0.516 845 609 396	-0.513 164 206 99	-0.509 744 252 7
43	-0.518 389 946 571 7	-0.514 574 386 104	-0.511 017 225 87	-0.507 724 683 2
44	-0.516 022 039 937 6	-0.512 330 629 670	-0.508 900 224 43	-0.505 738 379 5
45	-0.513 682 102 404 5	-0.510 116 997 691	-0.506 816 177 71	-0.503 788 806 7
46	-0.511 372 572 833 1	-0.507 936 193 030	-0.504 768 189 97	-0.501 879 706 3

Continued on Next Page...

Table 1 – Continuation

$L$	$v = 0$	$v = 1$	$v = 2$	$v = 3$
47	-0.509 095 905 143 5	-0.505 790 999 399	-0.502 759 557 97	-0.500 015 221 0
48	-0.506 854 594 707 7	-0.503 684 327 110	-0.500 793 858 28	-0.498 200 082 9
49	-0.504 651 210 969 6	-0.501 619 273 844	-0.498 875 073 34	-0.496 439 916 9
50	-0.502 488 438 936 8	-0.499 599 208 500	-0.497 007 783 09	-0.494 741 77
51	-0.500 369 133 705 2	-0.497 627 892 183	-0.495 197 476 73	-0.493 115 1
52	-0.498 296 394 825 7	-0.495 709 662 497	-0.493 451 107	
53	-0.496 273 672 262 6	-0.493 849 734 3	-0.491 778 2	
54	-0.494 304 925 576 7	-0.492 054 739		
55	-0.492 394 879 740	-0.490 333 83		
56	-0.490 549 476			

The ground state  $(L^\pi, v) = (0^+, 0)$  is well known and its value has been improved in several papers [3, 8, 2]. In particular Hijikata *et.al.* [5] reach an accuracy of 27 digits. In this sense we have an accuracy about  $10^{-13}$ .

Energies of the  $v = 0$  vibrational band for  $L = 2 - 12$  were presented by Zong *et.al.* [6]. Moss [1] presents not only non-adiabatic dissociation-energies but also relativistic and radiative corrections for bound vibrational states up to  $L = 5$ . Seven rovibrational states of the first electronic state are also presented there. More precise results for all the vibrational levels below the dissociation limit  $v \leq 27$  are given by Hilico *et.al.* [8] for the two lowest rotational quantum numbers  $L = 0, 1$ . Beyond that, Karr *et.al.* [9] extended this results until  $L = 2$  but with a different value of the deuteron mass  $m_d = 3670.4829652$ . In order to make some comparison with those results, Lagrange-mesh calculations considering this value of the deuteron mass are given in Table 2. Although less digits were obtained when comparing with [9] we can consider that the agreement is in all the digits presented.

The accuracies for the first, second and third rotational bands are  $10^{-11}$ ,  $10^{-10}$  and  $10^{-9}$ , respectively. The major comparison is possible with the results given by Moss [1]. The obtained spectrum is presented in Fig. 1.

Two cases of convergence tests are displayed in Table 3. For the values  $h = 0.14$  and  $h_z = 0.4$ , initial and final states are shown as well as the transition probability per second for different values of  $N$  and  $N_z$ . The transition probability  $W_0$  is obtained by restricting the matrix element (2) to the case where  $\kappa = 0$  while  $W_1$  corresponds to  $\kappa \leq 1$ . The  $\kappa = 1$  contributions have an importance smaller than 0.05 % and that the  $\kappa = 2$  contributions are smaller than 0.005 %. A good convergence with respect to  $N_z$  is already obtained for  $N_z = 20$ . The convergence with respect to  $N$  is slower. Since the convergence is exponential, one can estimate that the relative accuracy on  $W$  is about  $10^{-9}$  for  $(4^+, 0) \rightarrow (2^+, 0)$  and still better than  $10^{-8}$  for  $(43^-, 2) \rightarrow (35^-, 0)$ . Similar tests have been performed for other transitions.

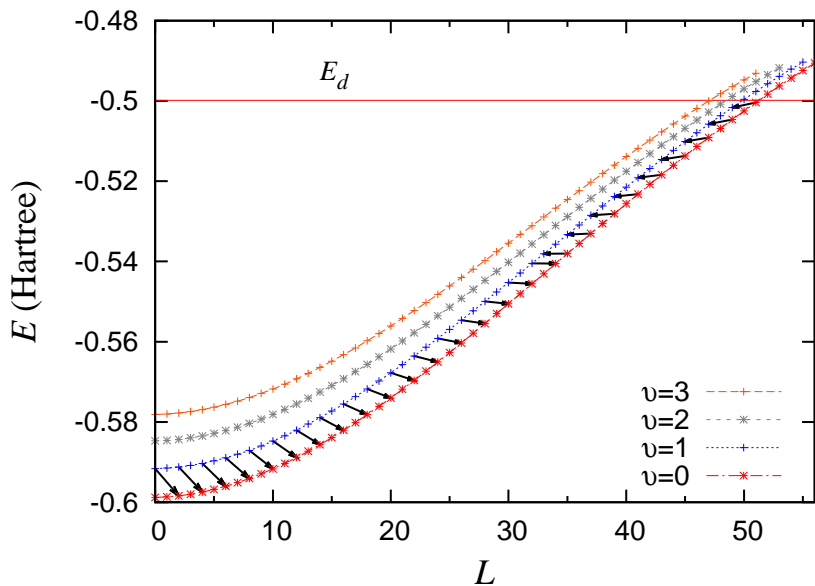


**Figure 1.** Four lowest  $\Sigma_g$  rotational bands of the  $D_2^+$  molecular ion and dissociation energy  $E_d$ . Arrows show how the direction of  $L \rightarrow L + 2$  transitions between the two lowest bands changes along the band.

**Table 2.** Comparison of the total energy for three rotational states  $L = 0 - 2$  and four vibrational states  $v = 0 - 3$  taking  $m_d = 3670.4829652$ . For each value of the rotational quantum number, the first line is calculated using the Lagrange mesh method with  $N = 45$  and  $N_z = 20$  and the scale factors are  $h = 0.08$  and  $h_z = 0.4$ . The second line are the results presented by Karr *et.al.*[9].

$L$	$v = 0$	$v = 1$	$v = 2$	$v = 3$
0	-0.598 788 784 304 46	-0.591 603 121 831 2	-0.584 712 206 896	-0.578 108 591 28
	-0.598 788 784 304 46	-0.591 603 121 831 23	-0.584 712 206 896 08	-0.578 108 591 28475
1	-0.598 654 873 192 5	-0.591 474 211 454 9	-0.584 588 169 503	-0.577 989 311 80
	-0.598 654 873 192 49	-0.591 474 211 454 95	-0.584 588 169 503 36	-0.577 989 311 80781
2	-0.598 387 585 778 5	-0.591 216 909 547 5	-0.584 340 598 262	-0.577 751 241 73
	-0.598 387 585 778 48	-0.591 216 909 547 45	-0.584 340 598 262 38	-0.577 751 241 73967

The convergence of the transition probabilities with respect to  $K_{\max}$  can be studied by comparison with results from wave functions truncated at  $K_{\max} = 0$  and  $K_{\max} = 1$ . The relative error when  $K_{\max} = 0$  is smaller than 0.3 for all considered transitions while the error for  $K_{\max} = 1$  is smaller than  $10^{-5}$ . This is rather similar to truncations with respect to  $\kappa$ . By extrapolation, we estimate that the relative error on the present transition probabilities obtained with  $K_{\max} = 2$  should be smaller than  $10^{-7}$ . The number of digits presented in Tables 4 and 5 are the same if we consider the deuteron mass as  $m_d = 3670.482962$ .

Table 4 presents the transitions probabilities per second for transitions within a same rotational band,  $L_f = L_i - 2$  and  $v_f = v_i \leq 3$ . They include some transition probabilities involving quasibound states. Six significant digits are given. These probabilities increase slowly with  $L$  with a maximum around  $L_i = 45, 43, 41$  and  $40$  for



**Table 3.** Convergence of the energies and transition probabilities as a function of the numbers  $N$  and  $N_z$  of mesh points. Two cases are shown:  $(4^+, 0) \rightarrow (2^+, 0)$  where  $L_f = L_i - 2$  (upper set) and  $(43^+, 3) \rightarrow (45^+, 1)$  where  $L_f = L_i + 2$  (lower set). The scale factors are  $h = 0.08$  and  $h_z = 0.4$ .

$N$	$N_z$	$E_i(4^+, 0)$	$E_f(2^+, 0)$	$W_0$ ( $10^{-11}\text{s}^{-1}$ )	$W_1$ ( $10^{-11}\text{s}^{-1}$ )	$W$ ( $10^{-11}\text{s}^{-1}$ )
20	20	-0.597 449 5	-0.598 379 6	2.97	2.97	2.97
30	20	-0.597 457 646 20	-0.598 387 585 24	2.966 273	2.965 657 294	2.965 657
30	30	-0.597 457 646 20	-0.598 387 585 24	2.966 273	2.965 657 295	2.965 657
40	20	-0.597 457 646 783 75	-0.598 387 585 809 95	2.966 271 937	2.965 656 618	2.965 656 329
40	30	-0.597 457 646 783 76	-0.598 387 585 809 97	2.966 271 938	2.965 656 618	2.965 656 329
45	20	-0.597 457 646 783 80	-0.598 387 585 809 99	2.966 271 937	2.965 656 618	2.965 656 329
50	20	-0.597 457 646 783 80	-0.598 387 585 809 99	2.966 271 937	2.965 656 618	2.965 656 329
$N$	$N_z$	$E_i(43^+, 2)$	$E_f(45^+, 0)$	$W_0$ ( $10^{-11}\text{s}^{-1}$ )	$W_1$ ( $10^{-11}\text{s}^{-1}$ )	$W$ ( $10^{-11}\text{s}^{-1}$ )
30	20	-0.507 54	-0.510 115 1	7.966 532	7.965 738	7.965 752
30	30	-0.507 54	-0.510 115 1	7.966 532	7.965 738	7.965 752
40	20	-0.507 724 681 4	-0.510 116 997 683	5.356 451 153	5.355 922 250	5.355 931 775
40	30	-0.507 724 681 4	-0.510 116 997 683	5.356 451 152	5.355 922 249	5.355 931 775
45	20	-0.507 724 683 174	-0.510 116 997 691 28	5.356 445 629	5.355 916 726	5.355 926 252
50	20	-0.507 724 683 184	-0.510 116 997 691 33	5.356 445 608	5.355 916 705	5.355 926 230

$v_i = 0, 1, 2$  and  $3$ , respectively, which is due to a maximum of the energy differences around  $L_i = 35$ .

Table 4: Quadrupole transition probabilities per second  $W$  for transitions between states of a same rotational band ( $v_f = v_i, L_f = L_i - 2$ ). Results are given with five digits followed by the power of 10.

$L_i$	$v_i = 0$	$v_i = 1$	$v_i = 2$	$v_i = 3$
2	3.066 49-13	3.069 47-13	3.041 09-13	2.983 89-13
3	5.026 89-12	5.028 74-12	4.979 40-12	4.883 07-12
4	2.965 66-11	2.964 08-11	2.932 50-11	2.873 43-11
5	1.086 42-10	1.084 55-10	1.071 79-10	1.049 07-10
6	3.012 58-10	3.003 01-10	2.963 57-10	2.896 89-10
7	6.952 82-10	6.918 74-10	6.816 71-10	6.652 88-10
8	1.408 15-09	1.398 48-09	1.375 27-09	1.339 80-09
9	2.585 58-09	2.562 15-09	2.514 33-09	2.444 51-09
10	4.397 74-09	4.347 29-09	4.256 29-09	4.128 87-09
11	7.033 38-09	6.934 41-09	6.772 21-09	6.553 53-09
12	1.069 24-08	1.051 23-08	1.023 87-08	9.882 24-09
13	1.557 73-08	1.526 92-08	1.482 93-08	1.427 32-08
14	2.188 42-08	2.138 42-08	2.070 56-08	1.987 05-08
15	2.979 43-08	2.901 83-08	2.800 88-08	2.679 62-08
16	3.946 54-08	3.830 72-08	3.685 31-08	3.514 39-08

Continued on Next Page...

Table 4 – Continuation

$L_i$	$v_i = 0$	$v_i = 1$	$v_i = 2$	$v_i = 3$
17	5.102 50-08	4.935 41-08	4.731 91-08	4.497 32-08
18	6.456 45-08	6.222 54-08	5.945 02-08	5.630 65-08
19	8.013 50-08	7.694 71-08	7.324 96-08	6.912 69-08
20	9.774 47-08	9.350 26-08	8.867 95-08	8.337 83-08
21	1.173 58-07	1.118 33-07	1.056 62-07	9.896 63-08
22	1.388 95-07	1.318 39-07	1.240 79-07	1.157 61-07
23	1.622 35-07	1.533 82-07	1.437 81-07	1.336 00-07
24	1.872 20-07	1.762 88-07	1.645 82-07	1.522 94-07
25	2.136 53-07	2.003 54-07	1.862 73-07	1.716 29-07
26	2.413 12-07	2.253 47-07	2.086 20-07	1.913 74-07
27	2.699 45-07	2.510 18-07	2.313 75-07	2.112 85-07
28	2.992 83-07	2.770 98-07	2.542 75-07	2.311 09-07
29	3.290 40-07	3.033 08-07	2.770 52-07	2.505 89-07
30	3.589 21-07	3.293 66-07	2.994 36-07	2.694 71-07
31	3.886 27-07	3.549 86-07	3.211 56-07	2.875 02-07
32	4.178 58-07	3.798 85-07	3.419 51-07	3.044 40-07
33	4.463 17-07	4.037 86-07	3.615 64-07	3.200 52-07
34	4.737 16-07	4.264 25-07	3.797 53-07	3.341 19-07
35	4.997 78-07	4.475 48-07	3.962 89-07	3.464 37-07
36	5.242 38-07	4.669 15-07	4.109 58-07	3.568 17-07
37	5.468 49-07	4.843 05-07	4.235 64-07	3.650 90-07
38	5.673 81-07	4.995 14-07	4.339 29-07	3.711 01-07
39	5.856 21-07	5.123 55-07	4.418 90-07	3.747 15-07
40	6.013 78-07	5.226 61-07	4.473 06-07	3.758 14-07
41	6.144 80-07	5.302 84-07	4.500 52-07	3.742 96-07
42	6.247 75-07	5.350 96-07	4.500 19-07	3.700 73-07
43	6.321 32-07	5.369 82-07	4.471 13-07	3.630 70-07
44	6.364 38-07	5.358 47-07	4.412 53-07	3.532 23-07
45	6.375 97-07	5.316 08-07	4.323 69-07	3.404 73-07
46	6.355 31-07	5.241 94-07	4.203 97-07	3.247 62-07
47	6.301 75-07	5.135 43-07	4.052 72-07	3.060 22-07
48	6.214 75-07	4.995 94-07	3.869 24-07	2.841 64-07
49	6.093 88-07	4.822 84-07	3.652 61-07	2.590 53-07
50	5.938 69-07	4.615 36-07	3.401 53-07	2.306 -07
51	5.748 75-07	4.372 43-07	3.113 89-07	1.98 -07
52	5.523 47-07	4.092 41-07	2.786 1 -07	
53	5.261 95-07	3.772 61-07	2.411 -07	
54	4.962 76-07	3.408 20-07		
55	4.623 36-07	2.990 -07		

Continued on Next Page...

Table 4 – Continuation

$L_i$	$v_i = 0$	$v_i = 1$	$v_i = 2$	$v_i = 3$
56	4.239 06-07			

Other transitions probabilities per second are given in Table 5. The columns correspond to transitions between different vibrational states. For each  $L_i$  value, the successive lines correspond to increasing values of  $L_f$ , i.e., to  $L_f = L_i - 2$  for  $L_i > 1$ ,  $L_f = L_i$  for  $L_i > 0$ , and  $L_f = L_i + 2$ , respectively. Comparison with previous results was not possible.

The strongest transition from each state occurs in general towards the nearest vibrational state ( $v_f = v_i - 1$ ). For  $v_f = v_i - 1$ , in the vicinity of  $L_i = 33$  and beyond, the  $(L_i, v_i) \rightarrow (L_i + 2, v_i - 1)$  transitions are replaced by  $(L_i + 2, v_i - 1) \rightarrow (L_i, v_i)$  transitions because the sign of the energy difference changes (see the arrows in Fig. 1 for the  $1 \rightarrow 0$  transitions). These numbers are indicated in italics in Table 5. For example, the first number in the last line for  $L_i = 33$  corresponds to the  $(35, 0) \rightarrow (33, 1)$  transition.

Table 5: Quadrupole transition probabilities per second  $W$  for transitions between different vibrational quantum numbers ( $v_i \neq v_f$ ). The three successive lines correspond to increasing  $L_f$  values, i.e.  $L_f = L_i - 2$ ,  $L_f = L_i$  and  $L_f = L_i + 2$ , respectively, for  $L_i \geq 2$ . Italicized numbers for  $(1 \rightarrow 0)$ ,  $(2 \rightarrow 1)$  and  $(3 \rightarrow 2)$  mean that the initial and final states are exchanged (the first one is preceded in each case by a horizontal bar).

$L_i$	(1 $\rightarrow$ 0)	(2 $\rightarrow$ 0)	(2 $\rightarrow$ 1)	(3 $\rightarrow$ 0)	(3 $\rightarrow$ 1)	(3 $\rightarrow$ 2)
0	7.461 27-08	7.384 89-09	1.301 15-07	5.354 45-10	2.012 70-08	1.693 82-07
1	3.521 48-08	4.090 47-09	6.120 20-08	3.738 19-10	1.100 72-08	7.940 26-08
	3.947 86-08	3.459 44-09	6.896 88-08	2.036 61-10	9.521 49-09	8.994 01-08
2	2.028 05-08	2.703 62-09	3.510 24-08	2.929 83-10	7.195 74-09	4.535 36-08
	2.506 41-08	2.918 23-09	4.355 33-08	2.673 17-10	7.851 42-09	5.649 51-08
	2.949 05-08	2.250 75-09	5.159 38-08	9.993 91-11	6.265 93-09	6.737 53-08
3	2.821 57-08	4.089 55-09	4.867 92-08	4.862 45-10	1.081 10-08	6.268 90-08
	2.326 86-08	2.718 68-09	4.042 32-08	2.499 09-10	7.312 65-09	5.242 05-08
	2.351 59-08	1.530 43-09	4.118 62-08	4.498 67-11	4.319 35-09	5.383 94-08
4	3.353 16-08	5.255 37-09	5.764 14-08	6.772 75-10	1.380 38-08	7.395 67-08
	2.250 34-08	2.641 49-09	3.908 07-08	2.439 32-10	7.102 60-09	5.066 09-08
	1.910 12-08	1.030 72-09	3.347 91-08	1.522 08-11	2.958 97-09	4.379 35-08
5	3.759 68-08	6.344 15-09	6.437 06-08	8.778 43-10	1.656 07-08	8.225 08-08

Continued on Next Page...

Table 5 – Continuation

$L_i$	(1 $\rightarrow$ 0)	(2 $\rightarrow$ 0)	(2 $\rightarrow$ 1)	(3 $\rightarrow$ 0)	(3 $\rightarrow$ 1)	(3 $\rightarrow$ 2)
	2.201 76-08	2.599 38-09	3.822 12-08	2.414 05-10	6.986 41-09	4.952 40-08
	1.556 44-08	6.702 08-10	2.729 11-08	2.052 48-12	1.967 06-09	3.570 98-08
6	4.079 56-08	7.386 00-09	6.953 87-08	1.089 20-09	1.916 43-08	8.844 93-08
	2.162 44-08	2.570 47-09	3.751 99-08	2.403 18-10	6.905 25-09	4.858 84-08
	1.263 83-08	4.112 04-10	2.216 18-08	5.740 85-13	1.244 14-09	2.899 63-08
7	4.325 41-08	8.379 90-09	7.337 19-08	1.309 22-09	2.161 46-08	9.285 51-08
	2.125 86-08	2.547 00-09	3.686 35-08	2.399 43-10	6.838 22-09	4.770 75-08
	1.019 14-08	2.306 67-10	1.786 58-08	7.284 93-12	7.300 41-10	2.336 53-08
8	4.501 22-08	9.313 39-09	7.594 90-08	1.534 21-09	2.388 16-08	9.558 41-08
	2.089 27-08	2.525 57-09	3.620 48-08	2.399 54-10	6.776 21-09	4.682 02-08
	8.144 51-09	1.117 79-10	1.426 82-08	1.944 82-11	3.811 20-10	1.864 51-08
9	4.608 15-08	1.016 96-08	7.730 22-08	1.759 57-09	2.592 47-08	9.669 47-08
	2.051 42-08	2.504 47-09	3.552 20-08	2.401 78-10	6.714 69-09	4.589 88-08
	6.441 16-09	4.103 09-11	1.127 27-08	3.486 89-11	1.623 01-10	1.471 28-08
10	4.646 90-08	1.093 08-08	7.745 83-08	1.980 23-09	2.770 14-08	9.624 14-08
	2.011 71-08	2.482 75-09	3.480 50-08	2.405 07-10	6.651 12-09	4.493 03-08
	5.035 63-09	7.109 49-12	8.800 46-09	5.179 80-11	4.410 20-11	1.146 75-08
11	4.618 86-08	1.158 01-08	7.645 75-08	2.191 01-09	2.917 28-08	9.429 78-08
	1.969 86-08	2.459 85-09	3.404 93-08	2.408 68-10	6.584 00-09	4.390 92-08
	3.887 87-09	4.400 59-13	6.782 31-09	6.887 70-11	1.435 85-12	8.819 54-09
12	4.526 64-08	1.210 32-08	7.436 18-08	2.386 87-09	3.030 67-08	9.096 67-08
	1.925 80-08	2.435 38-09	3.325 37-08	2.412 09-10	6.512 37-09	4.283 44-08
	2.961 63-09	1.297 61-11	5.154 90-09	8.509 09-11	1.307 78-11	6.686 30-09
13	4.374 24-08	1.248 89-08	7.125 79-08	2.563 16-09	3.107 95-08	8.638 31-08
	1.879 54-08	2.409 11-09	3.241 87-08	2.414 87-10	6.435 61-09	4.170 70-08
	2.223 72-09	3.806 67-11	3.860 00-09	9.972 33-11	6.135 35-11	4.991 40-09
14	4.167 09-08	1.272 98-08	6.725 64-08	2.715 82-09	3.147 81-08	8.071 16-08
	1.831 17-08	2.380 88-09	3.154 62-08	2.416 68-10	6.353 31-09	4.052 97-08
	1.643 92-09	7.034 14-11	2.844 30-09	1.123 11-10	1.318 72-10	3.664 63-09
15	3.911 91-08	1.282 26-08	6.248 90-08	2.841 51-09	3.149 95-08	7.414 24-08
	1.780 82-08	2.350 57-09	3.063 87-08	2.417 23-10	6.265 23-09	3.930 61-08
	1.195 04-09	1.055 89-10	2.059 72-09	1.225 99-10	2.132 39-10	2.642 37-09
16	3.616 52-08	1.276 80-08	5.710 46-08	2.937 76-09	3.115 12-08	6.688 50-08
	1.728 66-08	2.318 13-09	2.969 92-08	2.416 29-10	6.171 22-09	3.804 07-08
	8.529 71-10	1.406 25-10	1.463 51-09	1.304 97-10	2.967 38-10	1.868 03-09
17	3.289 57-08	1.257 07-08	5.126 39-08	3.002 94-09	3.045 02-08	5.916 10-08
	1.674 86-08	2.283 53-09	2.873 13-08	2.413 68-10	6.071 25-09	3.673 82-08

Continued on Next Page...

Table 5 – Continuation

$L_i$	(1 $\rightarrow$ 0)	(2 $\rightarrow$ 0)	(2 $\rightarrow$ 1)	(3 $\rightarrow$ 0)	(3 $\rightarrow$ 1)	(3 $\rightarrow$ 2)
	5.967 01-10	1.731 53-10	1.018 38-09	1.360 42-10	3.759 86-10	1.292 15-09
18	2.940 24-08	1.223 87-08	4.513 44-08	3.036 36-09	2.942 21-08	5.119 69-08
	1.619 63-08	2.246 77-09	2.773 86-08	2.409 26-10	5.965 34-09	3.540 38-08
	4.082 25-10	2.016 28-10	6.923 72-10	1.393 60-10	4.465 81-10	8.723 54-10
19	2.577 98-08	1.178 35-08	3.888 51-08	3.038 14-09	2.809 99-08	4.321 72-08
	1.563 17-08	2.207 88-09	2.672 49-08	2.402 91-10	5.853 59-09	3.404 28-08
	2.723 93-10	2.251 17-10	4.585 94-10	1.406 41-10	5.057 60-10	5.730 23-10
20	2.212 19-08	1.121 86-08	3.268 14-08	3.009 22-09	2.652 22-08	3.543 75-08
	1.505 69-08	2.166 92-09	2.569 41-08	2.394 57-10	5.736 16-09	3.266 04-08
	1.766 80-10	2.431 75-10	2.948 54-10	1.401 10-10	5.520 71-10	3.647 94-10
21	1.851 99-08	1.055 98-08	2.668 08-08	2.951 23-09	2.473 18-08	2.805 97-08
	1.447 41-08	2.123 94-09	2.465 01-08	2.384 19-10	5.613 24-09	3.126 22-08
	1.109 25-10	2.557 34-10	1.831 81-10	1.380 14-10	5.850 80-10	2.239 43-10
22	1.505 99-08	9.824 03-09	2.102 90-08	2.866 37-09	2.277 40-08	2.126 69-08
	1.388 54-08	2.079 02-09	2.359 68-08	2.371 77-10	5.485 06-09	2.985 35-08
	6.704 46-11	2.630 01-10	1.093 12-10	1.345 99-10	6.051 13-10	1.317 06-10
23	1.182 08-08	9.029 00-09	1.585 74-08	2.757 31-09	2.069 56-08	1.521 97-08
	1.329 29-08	2.032 28-09	2.253 80-08	2.357 32-10	5.351 90-09	2.843 94-08
	3.873 38-11	2.653 76-10	6.216 81-11	1.301 05-10	6.130 33-10	7.356 58-11
24	8.873 18-09	8.192 67-09	1.128 03-08	2.627 07-09	1.854 28-08	1.005 46-08
	1.269 86-08	1.983 80-09	2.147 75-08	2.340 88-10	5.214 04-09	2.702 52-08
	2.118 68-11	2.633 84-10	3.334 10-11	1.247 60-10	6.100 59-10	3.856 46-11
25	6.277 95-09	7.332 70-09	7.393 77-09	2.478 90-09	1.636 10-08	5.881 58-09
	1.210 45-08	1.933 72-09	2.041 88-08	2.322 50-10	5.071 81-09	2.561 57-08
	1.082 86-11	2.576 17-10	1.661 45-11	1.187 69-10	5.976 15-10	1.865 76-11
26	4.085 90-09	6.466 13-09	4.274 75-09	2.316 15-09	1.419 30-08	2.784 23-09
	1.151 26-08	1.882 13-09	1.936 56-08	2.302 27-10	4.925 53-09	2.421 57-08
	5.075 13-12	2.486 96-10	7.529 90-12	1.123 16-10	5.772 21-10	8.126 81-12
27	2.337 34-09	5.609 02-09	1.980 91-09	2.142 22-09	1.207 89-08	8.196 67-10
	1.092 46-08	1.829 18-09	1.832 09-08	2.280 27-10	4.775 54-09	2.282 97-08
	2.120 59-12	2.372 34-10	3.003 89-12	1.055 62-10	5.503 99-10	3.066 14-12
28	1.062 12-09	4.776 18-09	5.510 16-10	1.960 44-09	1.005 52-08	1.945 02-11
	1.034 24-08	1.774 98-09	1.728 81-08	2.256 59-10	4.622 18-09	2.146 18-08
	7.552 75-13	2.238 16-10	9.998 44-13	9.864 67-11	5.186 15-10	9.386 87-13
29	2.799 01-10	3.981 07-09	5.679 29-12	1.774 02-09	8.154 64-09	3.909 94-10
	9.767 44-09	1.719 66-09	1.627 01-08	2.231 34-10	4.465 80-09	2.011 62-08
	2.120 72-13	2.089 85-10	2.520 89-13	9.168 58-11	4.832 31-10	2.060 72-13

Continued on Next Page...

Table 5 – Continuation

$L_i$	(1 $\rightarrow$ 0)	(2 $\rightarrow$ 0)	(2 $\rightarrow$ 1)	(3 $\rightarrow$ 0)	(3 $\rightarrow$ 1)	(3 $\rightarrow$ 2)
30	7.032 29-13	3.235 64-09	3.485 02-10	1.586 00-09	6.405 90-09	1.919 30-09
	9.201 36-09	1.663 36-09	1.526 95-08	2.204 62-10	4.306 74-09	1.879 65-08
	4.021 25-14	1.932 27-10	3.927 23-14	8.477 62-11	4.454 82-10	2.447 20-14
31	2.255 30-10	2.550 31-09	1.567 42-09	1.399 23-09	4.833 62-09	4.568 97-09
	8.645 55-09	1.606 19-09	1.428 89-08	2.176 53-10	4.145 34-09	1.750 61-08
	3.509 86-15	1.769 73-10	2.144 34-15	7.799 62-11	4.064 60-10	6.198 47-16
32	9.471 79-10	1.933 95-09	3.636 24-09	1.216 31-09	3.458 43-09	8.286 36-09
	8.101 32-09	1.548 27-09	1.333 08-08	2.147 17-10	3.981 93-09	1.624 83-08
	2.962 28-17	1.605 94-10	1.306 19-18	7.140 81-11	3.671 06-10	<i>6.430 53-22</i>
33	2.151 10-09	1.394 00-09	6.516 22-09	1.039 62-09	2.297 18-09	1.300 18-08
	7.569 86-09	1.489 72-09	1.239 72-08	2.116 64-10	3.816 82-09	1.502 59-08
	<i>1.611 20-18</i>	1.443 99-10	<i>8.424 15-17</i>	6.506 00-11	3.282 16-10	<i>9.779 29-16</i>
34	3.816 28-09	9.364 63-10	1.015 77-08	8.712 85-10	1.363 18-09	1.863 16-08
	7.052 25-09	1.430 66-09	1.149 00-08	2.085 02-10	3.650 33-09	1.384 15-08
	<i>1.139 31-15</i>	1.286 46-10	<i>6.745 28-15</i>	5.898 76-11	2.904 43-10	<i>2.587 17-14</i>
35	5.916 19-09	5.661 05-10	1.450 18-08	7.132 37-10	6.665 25-10	2.508 06-08
	6.549 48-09	1.371 19-09	1.061 11-08	2.052 39-10	3.482 74-09	1.269 75-08
	<i>1.699 91-14</i>	1.135 40-10	<i>6.503 38-14</i>	5.321 66-11	2.543 11-10	<i>1.791 55-13</i>
36	8.419 63-09	2.865 40-10	1.948 18-08	5.671 93-10	2.144 55-10	3.224 34-08
	6.062 41-09	1.311 41-09	9.762 01-09	2.018 80-10	3.314 35-09	1.159 59-08
	<i>9.475 42-14</i>	9.923 81-11	<i>3.006 77-13</i>	4.776 40-11	2.202 22-10	<i>7.070 43-13</i>
37	1.129 16-08	1.004 02-10	2.502 46-08	4.347 06-10	1.174 03-11	4.000 66-08
	5.591 82-09	1.251 41-09	8.944 05-09	1.984 29-10	3.145 40-09	1.053 86-08
	<i>3.331 38-13</i>	8.585 86-11	<i>9.536 97-13</i>	4.263 96-11	1.884 75-10	<i>2.045 74-12</i>
38	1.449 42-08	9.504 00-12	3.105 20-08	3.172 01-10	6.109 78-11	4.824 99-08
	5.138 37-09	1.191 30-09	8.158 44-09	1.948 89-10	2.976 16-09	9.527 14-09
	<i>8.962 46-13</i>	7.348 19-11	<i>2.405 64-12</i>	3.784 75-11	1.592 73-10	<i>4.863 40-12</i>
39	1.798 70-08	1.501 27-11	3.748 19-08	2.160 20-10	3.636 02-10	5.684 75-08
	4.702 65-09	1.131 15-09	7.406 20-09	1.912 59-10	2.806 87-09	8.562 88-09
	<i>2.025 12-12</i>	6.215 76-11	<i>5.204 46-12</i>	3.338 74-11	1.327 39-10	<i>1.010 23-11</i>
40	2.172 82-08	1.176 26-10	4.422 92-08	1.324 80-10	9.191 03-10	6.566 87-08
	4.285 13-09	1.071 03-09	6.688 20-09	1.875 35-10	2.637 74-09	7.646 95-09
	<i>4.049 06-12</i>	5.190 88-11	<i>1.009 13-11</i>	2.925 52-11	1.089 27-10	<i>1.902 85-11</i>
41	2.567 48-08	3.177 61-10	5.120 63-08	6.794 19-11	1.726 63-09	7.457 85-08
	3.886 23-09	1.011 03-09	6.005 13-09	1.837 10-10	2.468 99-09	6.780 27-09
	<i>7.398 83-12</i>	4.273 64-11	<i>1.803 42-11</i>	2.544 42-11	8.783 41-11	<i>3.329 82-11</i>
42	2.978 34-08	6.157 51-10	5.832 39-08	2.389 56-11	2.784 81-09	8.343 71-08

Continued on Next Page...

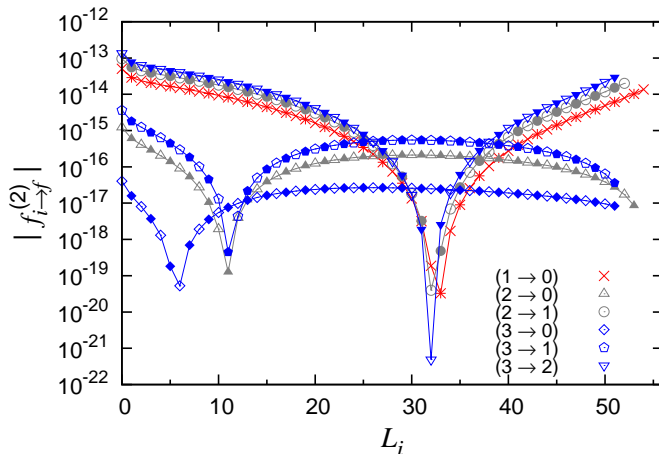
Table 5 – Continuation

$L_i$	(1 $\rightarrow$ 0)	(2 $\rightarrow$ 0)	(2 $\rightarrow$ 1)	(3 $\rightarrow$ 0)	(3 $\rightarrow$ 1)	(3 $\rightarrow$ 2)
	3.506 27-09	9.512 02-10	5.357 56-09	1.797 72-10	2.300 79-09	5.963 54-09
	<i>1.262 40-11</i>	3.462 31-11	<i>3.027 44-11</i>	2.194 56-11	6.940 82-11	<i>5.505 31-11</i>
43	3.401 01-08	1.012 05-09	6.549 09-08	2.062 35-12	4.092 21-09	9.209 92-08
	3.145 50-09	8.916 09-10	4.745 92-09	1.757 05-10	2.133 34-09	5.197 30-09
	<i>2.041 79-11</i>	2.753 65-11	<i>4.839 39-11</i>	1.874 94-11	5.355 93-11	<i>8.706 31-11</i>
44	3.831 15-08	1.507 46-09	7.261 45-08	4.531 33-12	5.647 71-09	1.004 13-07
	2.804 10-09	8.323 02-10	4.170 50-09	1.714 83-10	1.966 78-09	4.481 93-09
	<i>3.165 34-11</i>	2.143 26-11	<i>7.441 71-11</i>	1.584 44-11	4.016 57-11	<i>1.329 46-10</i>
45	4.264 40-08	2.103 40-09	7.959 94-08	3.393 63-11	7.450 75-09	1.082 15-07
	2.482 19-09	7.733 28-10	3.631 49-09	1.670 74-10	1.801 24-09	3.817 61-09
	<i>4.743 79-11</i>	1.625 82-11	<i>1.109 66-10</i>	1.321 92-11	2.908 09-11	<i>1.975 15-10</i>
46	4.696 48-08	2.802 13-09	8.634 65-08	9.369 47-11	9.501 41-09	1.153 27-07
	2.179 82-09	7.147 22-10	3.128 97-09	1.624 31-10	1.636 82-09	3.204 43-09
	<i>6.919 50-11</i>	1.195 28-11	<i>1.615 01-10</i>	1.086 19-11	2.013 85-11	<i>2.873 44-10</i>
47	5.123 08-08	3.607 18-09	9.275 08-08	1.883 36-10	1.180 02-08	1.215 46-07
	1.896 99-09	6.565 12-10	2.662 92-09	1.574 87-10	1.473 56-09	2.642 31-09
	<i>9.879 18-11</i>	8.450 64-12	<i>2.307 12-10</i>	8.760 65-12	1.315 56-11	<i>4.117 29-10</i>
48	5.539 92-08	4.523 64-09	9.869 73-08	3.239 54-10	1.434 67-08	1.266 30-07
	1.633 67-09	5.987 07-10	2.233 22-09	1.521 47-10	1.311 42-09	2.131 07-09
	<i>1.387 40-10</i>	5.681 54-12	<i>3.251 59-10</i>	6.903 90-12	7.934 92-12	<i>5.844 03-10</i>
49	5.942 57-08	5.558 60-09	1.040 54-07	5.088 20-10	1.713 62-08	1.302 65-07
	1.389 76-09	5.412 95-10	1.839 69-09	1.462 66-10	1.150 21-09	1.670 42-09
	<i>1.925 22-10</i>	3.571 82-12	<i>4.543 96-10</i>	5.280 29-12	4.264 14-12	<i>8.268 44-10</i>
50	6.326 40-08	6.721 46-09	1.086 61-07	7.541 0 -10	2.015 0 -08	1.320 1 -07
	1.165 13-09	4.842 28-10	1.482 07-09	1.396 0 -10	9.894 4 -10	1.260 0 -09
	<i>2.651 49-10</i>	2.044 26-12	<i>6.330 46-10</i>	3.878 8 -12	1.913 -12	<i>1.175 3 -09</i>
51	6.686 25-08	8.023 74-09	1.123 02-07	1.074 -09	2.333 -08	1.312 -07
	9.596 11-10	4.273 85-10	1.160 03-09	1.317 -10	8.28 -10	8.99 -10
	<i>3.641 53-10</i>	1.017 29-12	<i>8.849 45-10</i>	2.689 -12	6.24 -13	<i>1.69 -09</i>
52	7.015 89-08	9.476 8 -09	1.146 6 -07			
	7.730 11-10	3.705 1 -10	8.731 4 -10			
	<i>5.014 92-10</i>	4.030 2 -13	<i>1.252 4 -09</i>			
53	7.306 88-08	1.108 -08	1.151 6 -07			
	6.050 95-10	3.130 -10	6.2 -10			
	<i>6.975 09-10</i>	1.039 -13	<i>1.82 -09</i>			
54	7.545 71-08					
	4.555 87-10					

Continued on Next Page...

Table 5 – Continuation

$L_i$	(1 → 0)	(2 → 0)	(2 → 1)	(3 → 0)	(3 → 1)	(3 → 2)
	9.903	-10				

Figure 2. Oscillator strengths for  $L_f = L_i + 2$  transitions.

Figs. 2, 3 and 4 summarize the oscillator strengths for most of the considered transitions. For  $\Delta L = L_f - L_i = 2$  (Fig. 2) the oscillator strength has a strong variation along the band varying also with  $\Delta v = v_i - v_f$ . The strong minima for  $\Delta v = 1$  around  $L_i = 33$  are due to the change of sign of the energy difference (see Fig. 1). Beyond that value, the initial state is lower than the final  $v_f < v_i$  state and the strengths are negative. Otherwise the strengths slowly increase with the vibrational excitation. The  $\Delta v = 2$  strengths are smaller by more than an order of magnitude. The minimum occurring around  $L_i = 11$  is here due to a change of sign of the matrix element appearing in (2). The  $\Delta v = 3$  strengths are smaller by more than an order of magnitude than the  $\Delta v = 2$  strengths.

The  $\Delta L = 0$  oscillator strengths presented in Fig. 3 do not vary much along the bands. They slowly decrease for  $\Delta v = 1$  and slowly increase for  $\Delta v = 3$ . They are remarkably flat for  $\Delta v = 2$ .

The  $\Delta L = -2$  strengths presented in Fig. 4 behave similarly to the  $\Delta L = 2$  strengths. Minima take place around  $L_i = 29, 37$  and  $43$  for  $\Delta v = 1, 2$  and  $3$ , respectively. These minima thus occur now at increasing  $L_i$  values with increasing  $\Delta v$  and are all due to a change of sign of the matrix element.

The lifetimes can be calculated as

$$\tau = \left( \sum_{E_f < E_i} W_{i \rightarrow f} \right)^{-1}. \quad (10)$$

Using the transitions probabilities of Table 5 these are, for states with  $L = 0$   $1.340\,255 \times 10^7$ ,  $7.272\,729 \times 10^6$  and  $5.261\,929 \times 10^6$  for  $v = 1$ ,  $v = 2$  and  $v = 3$ , respectively. Lifetimes for the calculated states are displayed in Fig. 5.



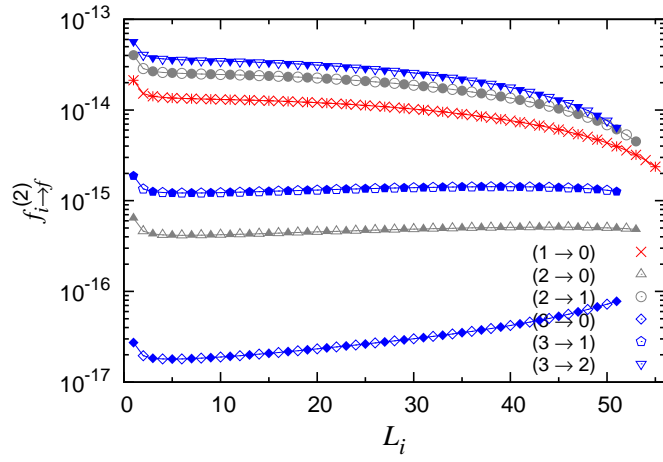


Figure 3. Oscillator strengths for  $L_f = L_i$  transitions.

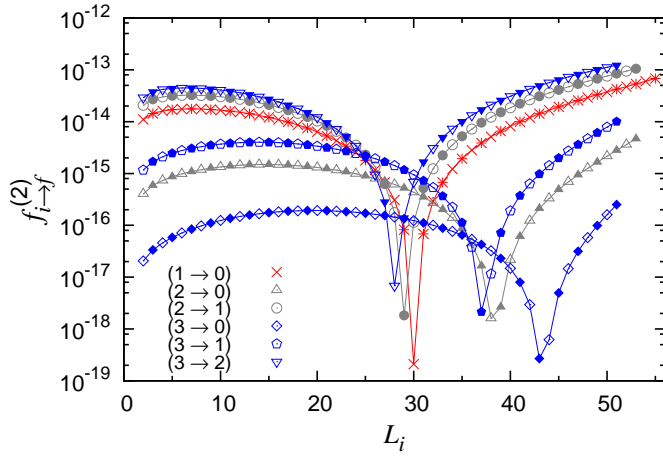


Figure 4. Oscillator strengths for  $L_f = L_i - 2$  transitions.

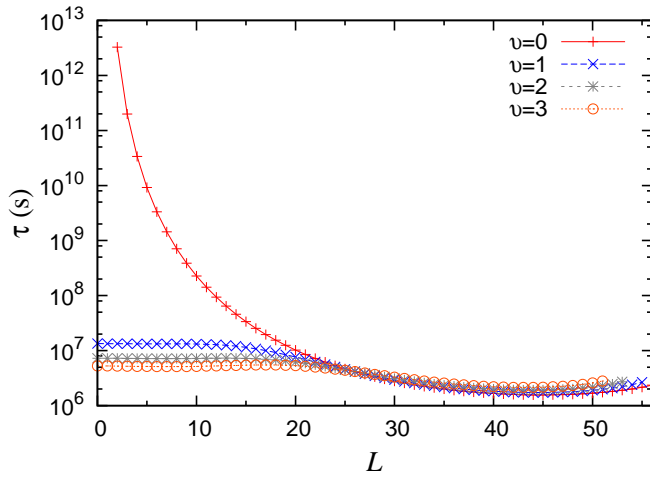


Figure 5. Lifetimes  $\tau$  in the first four rotational bands ( $v = 0 - 3$ ).

## 4. Conclusion

Applying the Lagrange-mesh method, the three-body Schrödinger equation for the deuterium molecular ion was solved with high precision in perimetric coordinates. Four vibrational states  $v = 0 - 3$  and  $L$  from 0 to 56 were considered. With the same number of mesh points in the  $x$  and  $y$  coordinates  $N = 40$  and  $N_z = 20$  for all the states considered, energies values are presented with 13 significant digits for the zero vibrational band until 9 significant digits for the third vibrational band.

With the wave functions provided by the Lagrange-mesh method, a simple calculation gives the quadrupole strengths and transition probabilities per time unit. Extensive tables and some figures are presented with six significant digits.

For high values of the total angular momentum  $L$  and  $\Delta v = 1$ , the initial and final states are interchange:  $L = 33, 33$  and  $32$  for  $v_i = 0 \rightarrow v_f = 1$ ,  $v_i = 1 \rightarrow v_f = 2$  and  $v_i = 2 \rightarrow v_f = 3$ , respectively. In comparison with the hydrogen molecular ion [12] this values are  $L = 23, 23$  and  $22$  for the same change in the vibrational bands. Also in a consistent way, quadrupole transitions for the deuterium molecular ion are less favorable than those for the hydrogen molecular ion, except for some values of the total angular momentum. As a consequence, lifetimes for  $D_2^+$  are greater than those for  $H_2^+$ . The difference is around one order of magnitude except for the states in the ground-state rotational band, roughly  $10^7$  and  $10^6$ , respectively.

## Acknowledgments

I indebted to D. Baye for initiating me into the subject and A. Turbinger for suggesting the problem and for their interest. I would like to thank the F.R.S.-FNRS (Belgium) for a postdoctoral grant.

## References

- [1] Richard E. Moss 1993 *J. Chem. Soc., Faraday Trans.* **89** 3851
- [2] Bailey D H and Frolov A M 2002 *J. Phys. B: At. Mol. Opt. Phys.* **35** 4287
- [3] Yan Z C, Zhang J Y and Li Y 2003 *Phys. Rev. A* **67** 062504
- [4] Moss R E 1999 *J. Phys. B: At. Mol. Opt. Phys.* **32** L89-L91
- [5] Hijikata Y, Nakashima H and Nakatsuji H 2009 *J. Chem. Phys.* **130** 024102
- [6] Yan Z C and Zhang J Y 2004 *J. Phys. B: At. Mol. Opt. Phys.* **37** 1055
- [7] Hesse M and Baye D 2003 *J. Phys. B: At. Mol. Opt. Phys.* **36** 139
- [8] Hilico L, Billy N, Grémaud B and Delande D 2000 *Eur. Phys. J. D* **12** 449
- [9] Karr J Ph and Hilico L 2006 *J. Phys. B: At. Mol. Opt. Phys.* **39** 2095
- [10] Hesse M and Baye D 1999 *J. Phys. B: At. Mol. Opt. Phys.* **32** 5605
- [11] Hesse M and Baye D 2001 *J. Phys. B: At. Mol. Opt. Phys.* **34** 1425
- [12] Horacio Olivares Pilón and Daniel Baye 2012 *J. Phys. B: At. Mol. Opt. Phys.* **45** 065101
- [13] Sobelman I I 1972 *An Introduction to the Theory of Atomic Spectra* (Pergamon, Oxford)
- [14] Sobelman I I 1979 *Atomic Spectra and Radiative Transitions* (Springer, Berlin)
- [15] Edmonds A R 1957 *Angular Momentum in Quantum Mechanics* (Princeton, New Jersey)
- [16] Moss R 1993 *Mol. Phys.* **80** 1541
- [17] Posen A, Dalgarno A and Peek J 1983 *At. Data Nucl. Data Tables* **28** 265

[18] Bollhöfer M and Notay Y 2007 *Comput. Phys. Commun.* **177** 951